

SYNTHETIC APERTURE RADAR IMAGING OF INTERNAL WAVES

An experiment to investigate synthetic aperture radar imaging of oceanic internal waves was conducted off the coast of Long Island in the late summer and early fall of 1984. Data acquired allow quantitative testing of model predictions for internal wave surface effects.

INTRODUCTION

Over the past 10 years, synthetic aperture radars (SAR) have frequently detected pronounced signatures of nonlinear, coastal internal waves¹⁻⁶ that are produced by the interaction of short-wavelength surface waves with internal wave-induced surface currents. A qualitative representation of the signature generation process is shown in Fig. 1 for a group of nonlinear internal waves. At the leading edge of each wave, there is a region of convergent flow that produces increased surface roughness; flow divergence at the trailing edge diminishes the surface roughness. The radar image consists of adjacent bright and dark bands, coincident with the rough and smooth regions, respectively, on a nearly uniform background associated with the mean local roughness.

In principle, it should be possible to combine a theoretical description for the internal wave/surface wave interaction process⁷ with a model for radar backscatter from the sea surface⁸ in order to compute the intensity of the SAR signatures and their dependence on environmental and imaging conditions. Unfortunately, most existing SAR images of internal waves have been obtained without the coincident *in situ* observations needed to characterize the internal wave properties and the surface wave conditions. Without such supporting information, it is not possible to assess the degree to which existing models can account for the features observed in the radar images.

To rectify the situation, the Office of Naval Research is sponsoring research efforts to investigate quantitatively the SAR imaging of oceanic internal wave surface effects. The centerpiece of the program is the SAR Internal Wave Signature Experiment (SARSEX), conducted in the New York Bight off the coast of Long Island in the late summer and early fall of 1984 using tidal-generated, nonlinear internal waves. This article summarizes the activities during SARSEX and presents some initial results.

SARSEX CONCEPT

The primary objectives of SARSEX are to investigate the basic hydrodynamic and electromagnetic mechanisms responsible for internal wave signatures

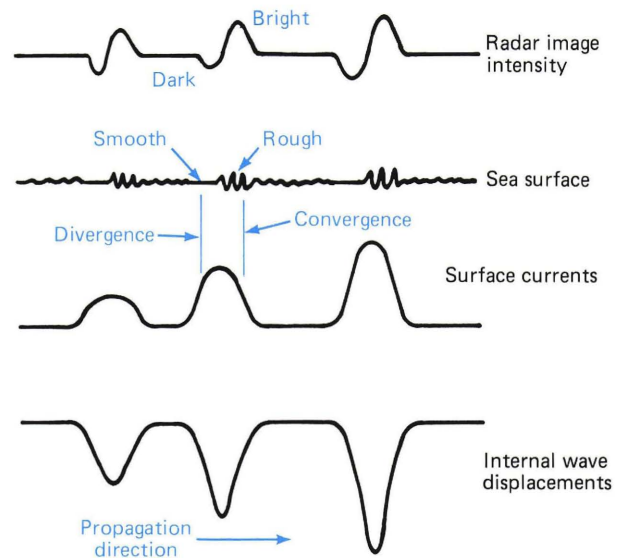


Figure 1—Schematic representation of the radar signature from a group of nonlinear internal waves. Alternating rough and smooth regions are produced on the sea surface by the internal wave currents. The roughness variations change the radar backscatter and appear as bright and dark features in a radar image.

in SAR images, to test available theories and models for quantitative predictions of SAR internal wave signatures, and to quantify the range of internal wave-induced current modulations that are observable in SAR images.

SARSEX is designed to be a rigorous examination of each major element in the SAR internal wave imaging process, shown schematically in Fig. 2. By melding measurements of internal wave characteristics with nonlinear internal wave models, analytical descriptions of the surface currents are produced for use as inputs to a wave-current interaction model. Measurements of surface wave modulations are then compared with predictions from the model to assess our understanding of the hydrodynamic processes contributing to the surface roughness variations. The roughness patterns in turn are input to radar backscatter models, and cross-section variations are calculated as part of a SAR

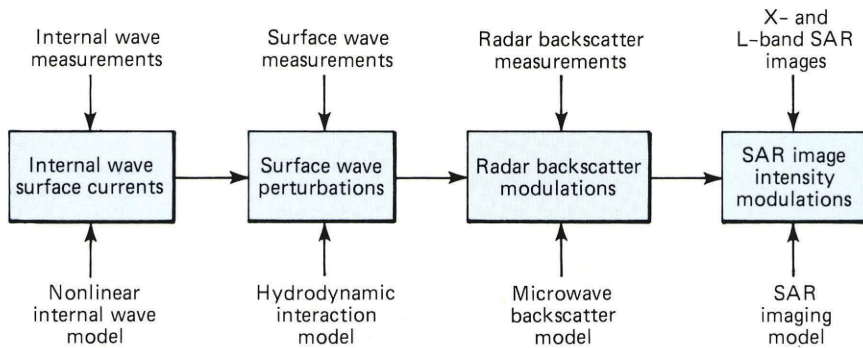


Figure 2—Imaging of an internal wave pattern with a synthetic aperture radar (SAR) involves hydrodynamic interactions between internal wave currents and surface waves, backscattering of microwave energy from the surface waves, and imaging effects due to scatterer motions during the aperture synthesis time. Measurements were obtained during the SAR Internal Wave Signature Experiment to test predictions from models for each stage in the imaging process.

imaging model that ultimately yields signature intensities for comparison with the actual SAR imagery. This procedure allows us to test independently both the hydrodynamic and the electromagnetic aspects of the SAR image formation process.

EXPERIMENT DESCRIPTION

SARSEX was conducted in two phases. During Phase I (August 27 to September 7, 1984), oceanographic measurements were made from the USNS *Bartlett* (a Navy research vessel) and the APL research vessel R/V *Cape*. Four current-meter moorings were also deployed to measure internal wave currents. Dual-frequency (X- and L-band) SAR imagery was obtained from a Convair CV-580 aircraft operated by the Canada Centre for Remote Sensing. Another Canadian CV-580 aircraft operated by the National Research Council flew a laser scatterometer. A third aircraft was used for low-altitude visual observation of the internal wave surface features. During Phase II (October 9-11, 1984), L-band SAR images of the SARSEX test

area were obtained from the space shuttle *Challenger* during the second Shuttle Imaging Radar (SIR-B) mission. These data were supported by oceanographic measurements from the R/V *Cape* and a single current-meter mooring. Table 1 summarizes the measurements obtained during both phases.

Phase I test operations were conducted within a 50 by 50 square kilometer area centered at 40 degrees north, 72 degrees 15 minutes west, on the continental shelf south of the eastern end of Long Island (Fig. 3). That area was selected because it is a known site of coherent, regularly produced internal waves that provide convenient test signals for systematic observations.⁹

Before the Phase I measurements were made, the R/V *Cape* made a brief survey of the test area to select sites for the current-meter moorings. Four moorings with a total of 11 two-axis acoustic current meters were deployed on August 20. The moorings were positioned in a rectangular pattern to provide information about the along-crest coherence of the internal waves

Table 1—Summary of SARSEX measurements.

<i>Date (1984)</i>	<i>Subsurface</i>	<i>Surface</i>	<i>Remote</i>
Phase I, Aug 27-Sep 7	Water velocity components (4 moorings, 11 current meters)	2-D surface slope wavenumber spectra (short waves)	X- and L-band backscatter (surface vessel)
	Isotherm displacements (thermistor chain)	Wave height spectra (long waves)	X- and L-band SAR imagery (aircraft)
	Conductivity and temperature profiles	Surface wind speed and direction	Optical backscatter (aircraft laser scatterometer)
	Echo sounder traces	Surface currents	
Phase II, Oct 9-11	Water velocity components (1 mooring, 2 current meters)	Wave height spectra	L-band SAR imagery (space shuttle)
	Conductivity and temperature profiles	Surface wind speed and direction	
	Echo sounder traces		

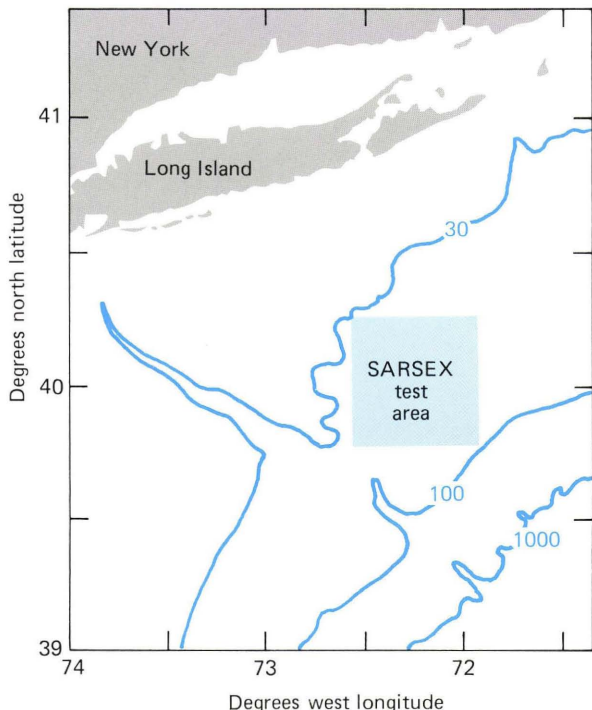


Figure 3—Location of SARSEX Phase I operations on the continental shelf south of Long Island. The bottom depth contours are in fathoms.

and their space-time evolution as they propagated shoreward.

The internal wave packets are generated near the shelf break, and they propagate toward the northwest at speeds of approximately 0.5 meter per second. The 200-kilohertz acoustic echo sounders on the research vessels were used to locate the wave packets and to determine their approximate propagation direction. Visual observations from a light aircraft confirmed the propagation direction and were used to survey nearby areas for wave activity.

After a packet was selected, *Bartlett* and *Cape* took positions approximately 1 kilometer apart and executed multiple racecourse tracks through the wave packet to acquire the subsurface and surface measurements (Fig. 4). Morning and afternoon data sessions took place on most days during Phase I. During eight of these sessions on seven different days, the SAR aircraft flew eight to ten passes over the test site to image the internal waves at different viewing geometries. Sixty-five internal wave SAR images were obtained. Also recorded were an additional 23 SAR images of calibration targets that were placed at an airport on Long Island. Coincident measurements with the laser scatterometer were obtained from the National Research Council's aircraft on four occasions.

Surface vessel positions were recorded using Loran-C navigation systems for track reconstruction, and position data for both CV-580 aircraft were obtained from the onboard inertial navigation systems.

During Phase II, three L-band SAR images of the SARSEX test area were acquired by the SIR-B radar

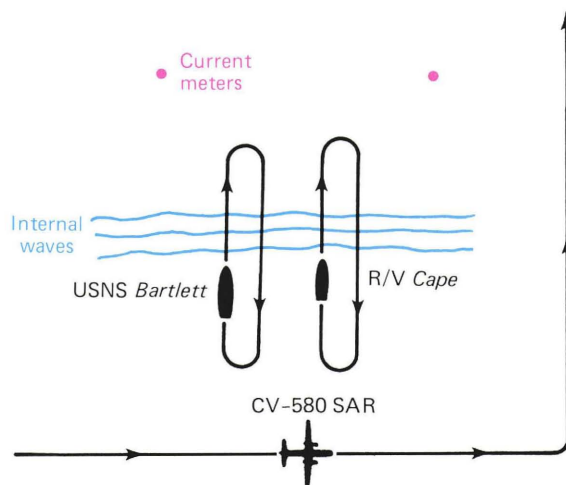


Figure 4—Typical measurement geometry during SARSEX. Both research vessels traversed an internal wave packet several times as it propagated past the current-meter moorings. Coincident SAR images were collected along different flight tracks to investigate signature dependencies on imaging geometry.

on the space shuttle. Supporting oceanographic data were obtained from the *R/V Cape* and a single current-meter mooring.

Principal investigators from several organizations participated in SARSEX. APL was responsible for the overall planning and conduct of the experiment and is charged with managing the reporting of results from the data analysis effort. It was also responsible for the oceanographic measurements required to characterize the environmental conditions, internal wave properties, surface currents, and surface wave perturbations induced by the internal waves. The Naval Ocean Research and Development Activity installed the current-meter moorings and processed the data records. Personnel from the Naval Research Laboratory obtained microwave backscatter measurements from a dual-frequency radar system on board *Bartlett*. The Environmental Research Institute of Michigan was responsible for the planning, acquisition, and calibration of the SAR imagery during SARSEX. A Canadian organization, the Defence Research Establishment Pacific, obtained internal wave signature measurements with an airborne laser scatterometer. The task of comparing the hydrodynamic and microwave measurements with predictions from numerical models describing the internal wave/surface wave interactions, radar backscatter phenomena, and the SAR imaging process is a joint undertaking involving APL, the Naval Research Laboratory, and the Environmental Research Institute of Michigan.

SAMPLE RESULTS

Results obtained from the analysis of one group of internal wave signatures from the Phase I operations are summarized in the remainder of this article. A more extensive discussion of the data and of the Phase

II results can be found in Ref. 10. Reference 11 reports on the SIR-B results from Phase II.

Figure 5 is a portion of the SAR images obtained during one aircraft pass on August 31. The internal waves of interest are the four prominent waves in the far range that are the leading waves in a packet moving toward the top of the image (305 degrees true). There is another group of internal waves in the vicinity of the research vessels that appears to be moving toward 335 degrees true. At the time of this image, the wind speed was 6 meters per second toward 90 degrees true.

Both the *Bartlett* and *Cape* crossed waves 2, 3, and 4 shortly after this SAR image was recorded, and the echo sounder trace from *Bartlett's* crossing is shown in Fig. 6. During the same crossing, images of the surface waves were recorded with video cameras in order to measure the surface wave roughness modulations induced by the internal waves. A dual-frequency (X- and L-band) radar scatterometer on the *Bartlett* also recorded backscatter modulations.

The R/V *Cape* towed a thermistor chain, consisting of 60 thermistors spaced 1 meter apart, during its crossing of waves 2, 3, and 4. The measurements yielded isotherm displacements (Fig. 7) from which internal wave amplitudes of 5 to 8 meters and wavelengths of approximately 200 meters were determined. Wave propagation speeds of 0.54 meter per second were computed from multiple crossings of these waves.

The procedure for estimating the surface currents was based on the known properties of nonlinear internal waves. The echo sounder and isotherm data were used to determine that the waves of interest can be treated as long-wavelength, mode 1, solitary waves. Accordingly, the isotherm displacement at a given depth z and time t is given by

$$H(x,z) = -A \operatorname{sech}^2 \phi(x) W_1(K,z), \quad (1)$$

where $\phi(x) = K(x - c_p t)$, which describes a thermocline depression moving at constant speed c_p . The function $W_1(K,z)$ is the mode 1 vertical eigenfunction obtained by solving the internal wave equation using the measured density profile and assuming no vertical current shear. The wavenumber K was estimated from the measurements and later verified by comparing the eigenfunction at this wavenumber with measured maximum displacements at different depths. A peak amplitude A was then calculated based on the depth of the displacement data relative to the depth of the predicted peak displacement obtained from the calculated eigenfunction.

The vertical distribution of the internal wave current is calculated from the vertical derivative of the eigenfunction; the horizontal dependence of the velocity is assumed to be identical with that of the displacement. Thus, the wave current $u(x,z)$ is given by

$$u(x,z) = -A c_p \operatorname{sech}^2 \phi(x) \frac{\partial W_1}{\partial z}. \quad (2)$$

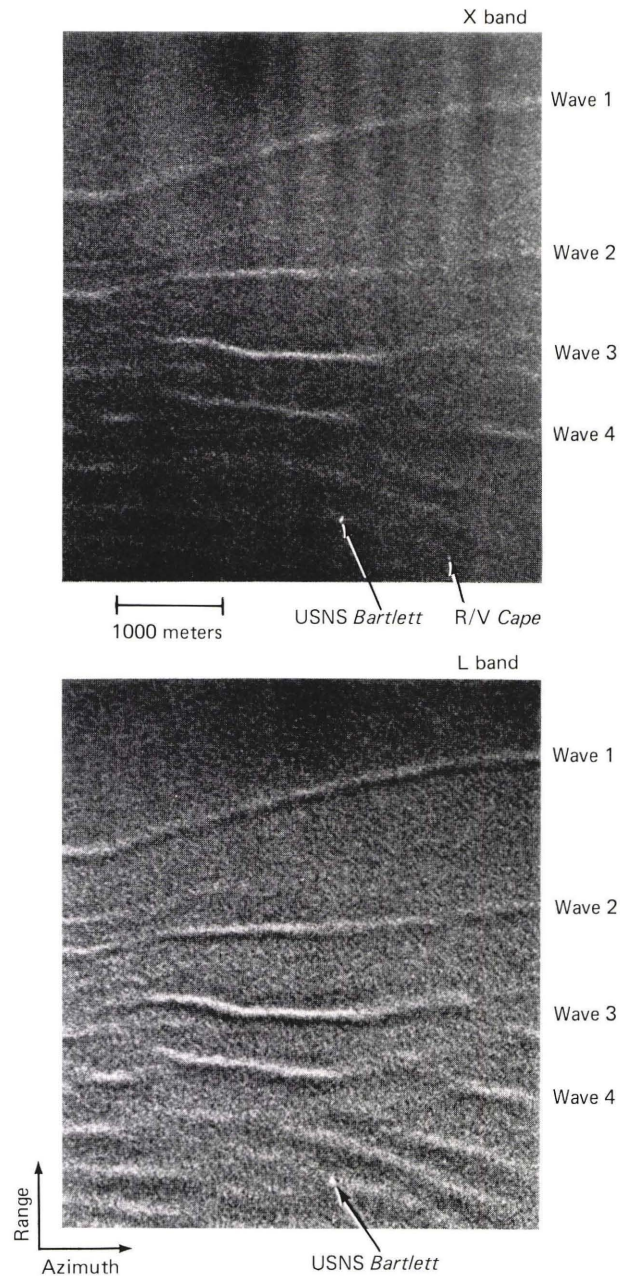


Figure 5—SAR images of an internal wave packet acquired during one aircraft pass on August 31. The bright streaks are due to increased radar backscatter from areas of enhanced surface wave roughness near the leading edge of each wave. The dark features indicate smooth regions where the surface currents have reduced the surface wave amplitudes. The research vessels, indicated by bright dots, proceeded toward the top of the image and crossed waves 4, 3, and 2 shortly after this image was recorded.

The surface strain rate $\partial u/\partial x$ is obtained by computing a horizontal derivative of the velocity at the surface.

$$\left(\frac{\partial u}{\partial x}\right)_{z=0} = 2AK c_p \left(\frac{\partial W_1}{\partial z}\right)_{z=0} \times \operatorname{sech}^2 \phi(x) \tanh \phi(x). \quad (3)$$

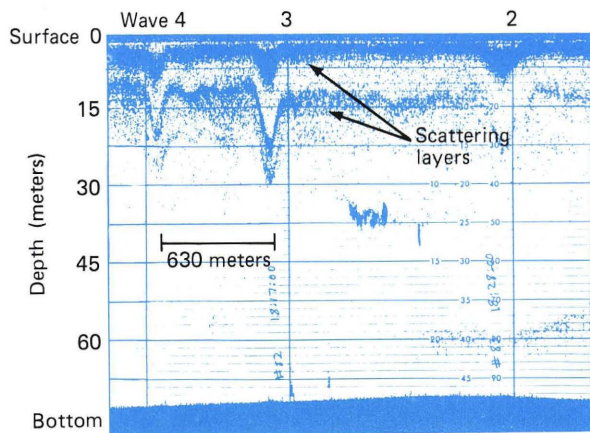
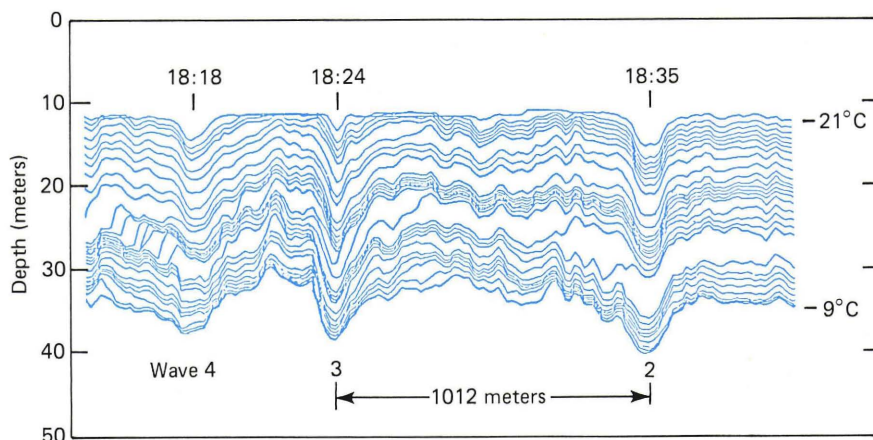


Figure 6—Acoustic echo sounder trace showing oscillations in the near-surface scattering layer during the crossing of waves 2, 3, and 4 by the USNS *Bartlett*.

Figure 8 shows the calculated surface currents and strain rates for waves 2, 3, and 4. The maximum surface currents range from 0.23 to 0.42 meter per second, and the maximum strain rates are 2.1 to 4.9×10^{-3} per second. Note the sign convention for the strain rate: negative strain corresponds to surface convergence whereas positive strain indicates divergence. The peak amplitudes computed for these waves are 5.6, 8.5, and 5.1 meters, respectively. The estimated nonlinear phase speed c_p is 0.7 meter per second.

The current-meter measurements provide an independent check of the calculations since the predicted wave current depth profile can be compared with the measured currents at the depths of the current meters. Near the time of the SAR measurements, the wave packet passed one of the moorings; the wave currents at an 18-meter depth are shown in Fig. 9. The current magnitudes were computed after filtering the tidal signal from the measured velocity components. The predicted velocity profiles and the measured currents were in good agreement, validating our approach for combining measurements with a nonlinear internal wave model to estimate the surface currents and strain rates.

Figure 7—Isotherm variations from waves 4, 3, and 2 recorded with the thermistor chain towed by the R/V *Cape*.



SURFACE WAVE MODULATIONS

Video images of the surface waves were recorded using charge-coupled device television cameras mounted on the bow of the *Bartlett*. Under proper illumination conditions, the brightness in these images can be related to the slopes of the surface waves. To quantify the surface wave modulations induced by the internal waves, the images are digitized and processed to generate two-dimensional wavenumber slope spectra as a function of position in the internal wave packet. Before encountering an internal wave, the image spectrum represents the undisturbed background wave field. As the vessel overtakes the internal wave, the spectrum first decreases and then increases before returning to the background level, reflecting the reduction and increase in surface wave energy caused by the internal wave current pattern (Fig. 1). In addition to the amplitude changes, there is also a rotation of the spectrum induced by the current. An extensive analysis is in progress to compare the observed spectrum changes with predictions from the wave-current interaction model in order to test directly the adequacy of our understanding of these hydrodynamic effects.

SAR SIGNATURES

X- and L-band SAR images were recorded on both optical and digital recorders throughout the experiment. All of the signal film has been optically processed by the Environmental Research Institute of Michigan, and the imagery is used to survey the database. Specific images selected for detailed analysis are generated from the digital database, and calibration factors are applied to relate image intensity variations to changes in cross section.¹²

To quantify the internal wave SAR signatures, average intensity traces are computed along linear segments normal to the internal wave crests. The intensity scans are typically averaged over approximately 150 meters in the cross-wave direction and then further smoothed over 30 meters in the propagation direction to reduce speckle noise. For the imaging geometry shown in Fig. 5 where the internal waves are propagating toward the top of the image, the intensity traces were oriented ver-

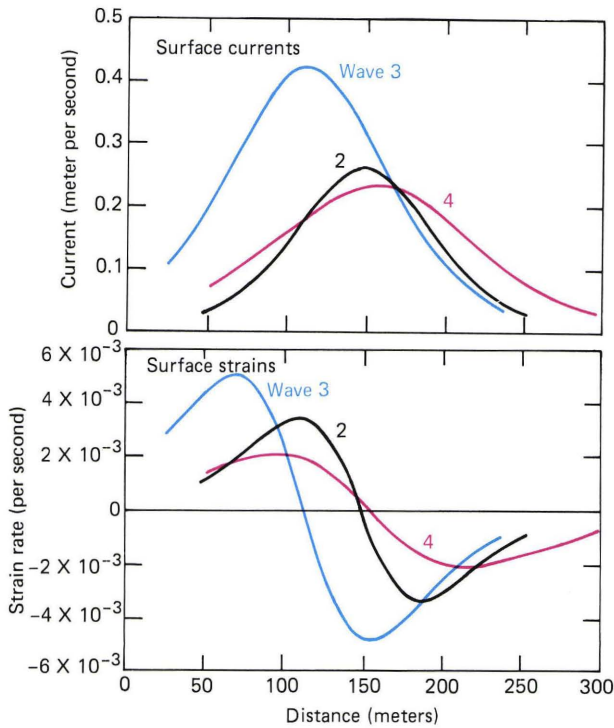


Figure 8—Surface currents and horizontal current gradients, or strain rates, computed from oceanographic measurements and the nonlinear internal wave model.

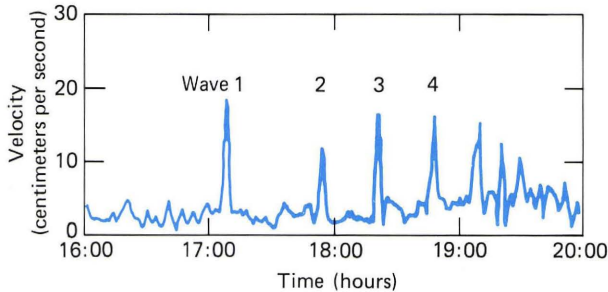


Figure 9—Internal wave currents at a depth of 18 meters recorded as the wave packet passed a current-meter mooring.

tically and centered along the ground tracks of the research vessels. Figure 10 shows the results from traces along the *Bartlett's* track in Fig. 5. Here the radar noise level has been subtracted, the mean signal decrease with increasing range has been removed, and the background intensity has been normalized to unity to display the internal wave signals relative to the local background return.

Several characteristics of the internal wave signatures should be noted. First, the L-band image (Fig. 5) shows distinct bright features followed by a dark region, consistent with our expectation (Fig. 1). The X-band image, however, exhibits only bright features. Second, the L-band signature intensities are 1.5 to 3 times larger than the mean background level; the X-band signals are slightly smaller, ranging from 1.25 to 2.75 times background. Third, by carefully register-

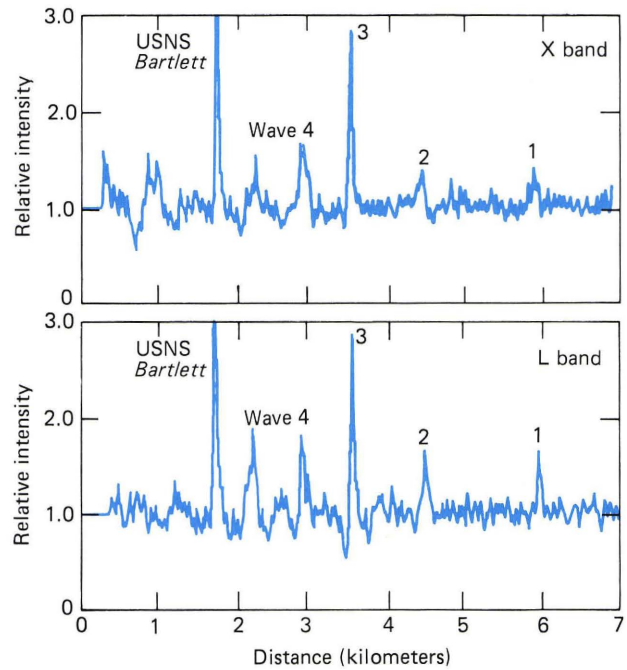


Figure 10—SAR image intensity variations along the track of the USNS *Bartlett* in Fig. 5. The large return from the *Bartlett* has been clipped in this plot to display the lower amplitude internal wave features.

ing the X- and L-band images, it has been found that the bright features in both images correspond to the same part of the internal wave. A successful SAR imaging model must account for these observations.

A detailed discussion of the wave-current interaction model and the calculations done to produce SAR image intensity predictions for these internal waves appear in an article by Thompson elsewhere in this issue. The signature predictions were made by using a hydrodynamic model for the interaction of internal wave currents and ambient surface waves and by assuming that the microwave backscattered power was caused by Bragg scattering. Inputs to the hydrodynamic model included the internal wave surface current, phase speed, and propagation direction; a model equilibrium surface wave spectrum appropriate for the measured wave and wind conditions; and a model function for the surface wave relaxation time. Figure 11 shows a comparison of the predicted L-band SAR intensity variations with the measured intensities for waves 2, 3, and 4. The predicted signals agree with the general shape of the observations, but the bright features are generally underpredicted by a factor of 2 to 3. When the same model is applied to the X-band internal wave signatures, we find that the predicted signals are an order of magnitude smaller than those observed.

The results are interpreted as evidence that the hydrodynamic description of the wave-current interaction process is essentially correct for surface waves with wavelengths of 20 to 30 centimeters, since these waves produce the L-band radar backscatter. The failure of the model to predict the X-band signals indi-

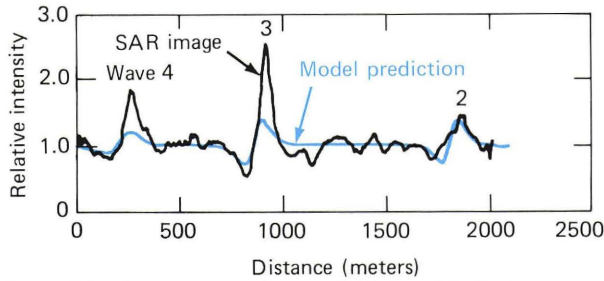


Figure 11—Comparison of predicted L-band SAR signatures from waves 4, 3, and 2 with measured image intensity variations along the track of the USNS *Bartlett*.

cates that our interaction model lacks some of the essential physics contributing to the surface roughness modulation of the 2- to 3-centimeter surface waves that are responsible for the X-band backscatter. These conclusions are elaborated further in the article by Thompson.

CONCLUSION

A large body of data on the hydrodynamic properties and electromagnetic signatures of continental shelf internal waves was obtained during SARSEX under a variety of wind, surface wave, and radar illumination conditions. Results obtained to date have delineated some areas where existing theories appear adequate to account for the observed radar signatures; the results have also highlighted areas where theoretical developments are needed. Additional data from work in progress should lead to an improved understanding of radar imaging of internal waves.

THE AUTHORS

RICHARD F. GASPAROVIC (center) is the supervisor of the Remote Sensing Group in the Submarine Technology Department. He received a B.S. degree from Fordham University in 1963 and graduate degrees in physics from the University of Pennsylvania (M.S., 1964) and Rutgers (Ph.D., 1969). He was employed by RCA briefly before joining APL in 1971.

Dr. Gasparovic has been associated with several research efforts involving remote sensing of the ocean surface. His research interests include infrared sensing of sea surface temperature, optical measurements of surface wave properties, and microwave manifestations of oceanic processes.

ALAN BRANDT (left) is a group scientist in the Hydrodynamics Group and a senior scientist at the Chesapeake Bay Institute. He received the B.C.E. degree from the Cooper Union (1959) and the M.S.C.E. (1963) and Ph.D. (1966) degrees in civil engineering and fluid dynamics from Carnegie Mellon University. In 1965, he joined APL, where he worked on the fluid dynamics and combustion of missile propulsion systems and on the flywheel energy-storage program. During 1971, Dr. Brandt was at Imperial College, London, where he did research in turbulent flow. Since his return, he has been engaged in laboratory modeling of hydrodynamic flows and ocean data analysis for the Submarine Security Technology Program. Most recently, he has been involved in developing multidisciplinary programs on estuarine and coastal oceanography, initially focusing on the Chesapeake Bay.

REFERENCES

- 1 C. Elachi and J. R. Apel, "Internal Wave Observations Made with an Airborne Synthetic Aperture Imaging Radar," *Geophys. Res. Lett.* **3**, 647 (1976).
- 2 W. Alpers and E. Salusti, "Scylla and Charybdis Observed from Space," *J. Geophys. Res.* **88**, 1800-1808 (1983).
- 3 J. R. Apel and F. I. Gonzalez, "Nonlinear Features of Internal Waves off Baja California as Observed from the Seasat Imaging Radar," *J. Geophys. Res.* **88**, 4459-4466 (1983).
- 4 B. A. Hughes and J. F. R. Gower, "SAR Imagery and Surface Truth Comparisons of Internal Waves in Georgia Strait, British Columbia, Canada," *J. Geophys. Res.* **88**, 1809-1824 (1983).
- 5 R. P. Trask and M. G. Briscoe, "Detection of Massachusetts Bay Internal Waves by the Synthetic Aperture Radar (SAR) on Seasat," *J. Geophys. Res.* **88**, 1789-1799 (1983).
- 6 L.-L. Fu and B. Holt, "Internal Waves in the Gulf of California: Observations from a Spaceborne Radar," *J. Geophys. Res.* **89**, 2053-2060 (1984).
- 7 B. A. Hughes, "The Effect of Internal Waves on Surface Wind Waves, 2. Theoretical Analysis," *J. Geophys. Res.* **83**, 455-465 (1978).
- 8 G. R. Valenzuela, "Theories for the Interaction of Electromagnetic and Oceanic Waves—A Review," *Boundary-Layer Meteorol.* **13**, 61-85 (1978).
- 9 J. R. Apel, H. M. Byrne, J. R. Proni, and R. L. Charnell, "Observations of Oceanic Internal and Surface Waves from the Earth Resources Technology Satellite," *J. Geophys. Res.* **80**, 865-881 (1975).
- 10 SARSEX Experiment Team, *SARSEX Interim Report*, JHU/APL STD-R-1200 (1985).
- 11 R. F. Gasparovic, J. R. Apel, D. R. Thompson, and J. S. Tochko, "A Comparison of SIR-B Radar Data with Internal Wave Measurements via a SAR Imaging Theory" (submitted to *Science*, 1985).
- 12 E. S. Kasischke et al., *SAR Data Collection and Processing Summary—1984 SARSEX Experiment*, ERIM Report 155900-21-T (1985).

ACKNOWLEDGMENTS—Numerous individuals at several organizations contributed to the success of SARSEX. We especially thank the following: S. Babin, D. Dubbel, B. Gotwols, J. Hansen, J. Hillier, G. Keys, R. Miller, L. Peterson, J. Rowland, W. Sparrow, J. Tochko, and R. Whiting of APL; B. Hughes and S. Hughes of the Defence Research Establishment Pacific; R. Shuchman of the Environmental Research Institute of Michigan; A. Green and D. Burns of the Naval Ocean Research and Development Activity; and D. Schuler of the Naval Research Laboratory. This work was sponsored by the Office of Naval Research.

JOHN R. APEL's biography can be found on p. 336.



ERIC S. KASISCHKE was born in St. Joseph, Mich., in 1952 and is now completing work toward a Ph.D. degree from the University of Michigan. He has been employed in the Radar Division of the Environmental Research Institute of Michigan since 1976. Prior to that, he worked for the Institute of Social, Economic and Government Research of the University of Alaska.

Mr. Kasischke's research interests are in the detection of oceanic processes on synthetic aperture radar imagery. Over the past several years, he has directed aircraft flight operations during several major SAR/oceanographic experiments and has conducted research on Seasat, SIR-A, and aircraft SAR data.

